

Regional analysis of annual maximum rainfall using TL-moments method

Ani Bin Shabri · Zalina Mohd Daud ·
Noratiqah Mohd Ariff

Received: 11 January 2010 / Accepted: 23 March 2011 / Published online: 26 April 2011
© Springer-Verlag 2011

Abstract Information related to distributions of rainfall amounts are of great importance for designs of water-related structures. One of the concerns of hydrologists and engineers is the probability distribution for modeling of regional data. In this study, a novel approach to regional frequency analysis using L-moments is revisited. Subsequently, an alternative regional frequency analysis using the TL-moments method is employed. The results from both methods were then compared. The analysis was based on daily annual maximum rainfall data from 40 stations in Selangor Malaysia. TL-moments for the generalized extreme value (GEV) and generalized logistic (GLO) distributions were derived and used to develop the regional frequency analysis procedure. TL-moment ratio diagram and Z-test were employed in determining the best-fit distribution. Comparison between the two approaches showed that the L-moments and TL-moments produced equivalent results. GLO and GEV distributions were identified as the most suitable distributions for representing

the statistical properties of extreme rainfall in Selangor. Monte Carlo simulation was used for performance evaluation, and it showed that the method of TL-moments was more efficient for lower quantile estimation compared with the L-moments.

1 Introduction

Extreme environmental events, such as high-intensity rains and floods, can have substantial impacts on society and the economy. The estimation of their return periods and the magnitude of extreme event are of great importance in hydrologic modeling, reservoir management, and also design of hydraulic structures such as bridges, dams, spillways, culverts, and irrigation ditches.

In a relatively young country like Malaysia, annual rainfall or river flow records are all too often inadequate or unavailable to allow for reliable estimation of extreme events at a location of interest. This poses a difficulty for hydrologist or engineers to derive reliable flood estimates. Therefore, estimation using regional frequency analysis is a popular and practical means of providing flood information at stations with little or no flow data available for the purposes of flood control and engineering economic (Jingyi and Hall 2004).

Hosking and Wallis (1997) have developed a new approach to regional frequency analysis based on L-moments. This technique has been used at all stages of regional analysis including the identification of homogeneous regions, identification and testing of regional frequency distributions, and estimations of flood quantiles at stations of interest. The approach has been applied successfully in modeling floods in a number of cases

A. B. Shabri (✉)
Department of Mathematics, Faculty of Science,
Universiti Teknologi Malaysia,
81310 Skudai, Johor, Malaysia
e-mail: ani@utm.my

Z. M. Daud
UTM Razak School of Engineering and Advanced Technology,
Universiti Teknologi Malaysia International Campus,
50300 Kuala Lumpur, Malaysia

N. M. Ariff
School of Mathematical Science,
Faculty of Science and Technology,
National University of Malaysia,
43600 Bangi, Selangor, Malaysia

Table 1 Parameter development for the GLO, GEV, and GPA distributions

Distribution	TL-moments and TL-moment ratio	Parameter estimates
GLO	$\lambda_1^{(1)} = \frac{\alpha}{k} + \xi - \frac{\pi\alpha(1-k^2)}{\sin(\pi k)}$	$\hat{k} = \frac{-9\hat{\tau}_3^{(1)}}{5}$
	$\lambda_2^{(1)} = -\frac{\pi\alpha k(k^2-1)}{2\sin(\pi k)}$	$\hat{\alpha} = -\frac{2\hat{\lambda}_2^{(1)}\sin(\pi\hat{k})}{\pi\hat{k}(\hat{k}^2-1)}$
	$\tau_3^{(1)} = -\frac{5k}{9} \quad \tau_4^{(1)} = \frac{7k^2+2}{24}$	$\hat{\xi} = \hat{\lambda}_1^{(1)} + \frac{\pi\hat{\alpha}(1-\hat{k}^2)}{\sin(\pi\hat{k})} - \frac{\hat{\alpha}}{\hat{k}}$
GEV	$\lambda_1^{(1)} = \xi + \frac{\alpha}{k} [1 - \Gamma(1+k)(\frac{3}{2k} - \frac{2}{3k})]$	$\hat{k} = 0.2816 - 2.8825\hat{\lambda}_3^{(1)} + 1.3744(\hat{\lambda}_3^{(1)})^2 - 0.8462(\hat{\lambda}_3^{(1)})^3$
	$\lambda_2^{(1)} = 6\alpha\Gamma(k)(\frac{1}{2(4k)} - \frac{1}{3k} + \frac{1}{2(2k)})$	$\hat{\alpha} = \frac{\hat{\lambda}_2^{(1)}}{6\Gamma(\hat{k})(\frac{1}{2(4\hat{k})} - \frac{1}{3\hat{k}} + \frac{1}{2(2\hat{k})})}$
	$\tau_3^{(1)} = \frac{10(\frac{1}{3k} - \frac{5}{2(4k)} + \frac{2}{3k} - \frac{1}{2(2k)})}{9(\frac{1}{2(4k)} - \frac{1}{3k} + \frac{1}{2(2k)})}$	$\hat{\xi} = \hat{\lambda}_1^{(1)} - \frac{\hat{\alpha}}{\hat{k}} [1 - \Gamma(1+\hat{k})(\frac{3}{2k} - \frac{2}{3k})]$
	$\tau_4^{(1)} = \frac{5(\frac{7}{3(6k)} - \frac{7}{5k} + \frac{15}{2(4k)} - \frac{10}{3(3k)} + \frac{1}{2(2k)})}{4(\frac{1}{2(4k)} - \frac{1}{3k} + \frac{1}{2(2k)})}$	
GPA	$\lambda_1^{(1)} = \xi + \frac{(k-5)\alpha}{(k+2)(k+3)}$	$\hat{k} = \frac{10-45\hat{\tau}_3^{(1)}}{10+9\hat{\tau}_3^{(1)}}$
	$\lambda_2^{(1)} = \frac{6\alpha}{(k+2)(k+3)(k+4)}$	$\hat{\alpha} = \frac{\hat{\lambda}_2^{(1)}}{6} (\hat{k}+2)(\hat{k}+3)(\hat{k}+4)$
	$\tau_3^{(1)} = \frac{10(1-k)}{9(k+5)} \quad \tau_4^{(1)} = \frac{5\alpha(k-1)(k-2)}{4(k+5)(k+6)}$	$\hat{\xi} = \hat{\lambda}_1^{(1)} - \frac{(\hat{k}-5)\hat{\alpha}}{(\hat{k}+2)(\hat{k}+3)}$

studied in Malaysia (Lim and Lye 2003), New Zealand (Madsen et al. 1997), Southern Africa (Kjeldsen et al. 2002), Turkey (Saf 2010), Iran (Rahnama and Rostami 2007), China (Chen et al. 2006), Italy (Noto and La Loggia 2009; Cannarozzo et al. 2009), Pakistan (Hussain and Pasha 2009), Tunisia (Abida and Ellouze 2008), Canada (Glaves and Waylen 1997; Yue and Wang 2004), UK (Fowler and Kilsby 2003), and India (Parida et al. 1998; Kumar et al. 1999, 2003a).

Elamir and Seheult (2003) introduced trimmed L-moments (TL-moments) which are a generalization of L-moments. TL-moments have certain advantages over L-moments and conventional moments. TL-moments which assign zero weight to extreme observations are practically easy to compute and are more robust compared with L-moments when used to estimate from

a sample containing outliers. However, as observed from the literature, TL-moments have not been widely applied in frequency analysis. At present, TL-moments have only been derived for the normal, logistic, Cauchy, exponential, and generalized pareto (GPA) distributions (Elamir and Seheult 2003).

Many statistical distributions for regional frequency analysis have been investigated for extreme hydrologic variables. In this study, three probability distributions were considered: generalized extreme value (GEV), generalized logistic (GLO), and GPA. The short-listed distributions were chosen based on previous studies such as those by Zin et al. (2009) and Zalina et al. (2002) of which these distributions were more prominent for tropical regions and by Kysely (2009) for modeling precipitation extremes. This paper aims to provide a comprehensive evaluation of the L-

Table 2 Equation coefficient of TL-moment ratio for the GEV, GPA, and GLO distributions

Corresponding equation: $\tau_4^{DIS} = \alpha_0 + \alpha_1\tau_3^{(1)} + \alpha_2(\tau_3^{(1)})^2 + \alpha_3(\tau_3^{(1)})^3 + \alpha_4(\tau_3^{(1)})^4$					
Distribution	α_0	α_1	α_2	α_3	α_4
GEV	0.0576	0.0942	0.9183	-0.0745	0.0373
GPA	0	0.1610	0.9904	-0.1295	0.0184
GLO	0.0833	0	0.9450	0	0

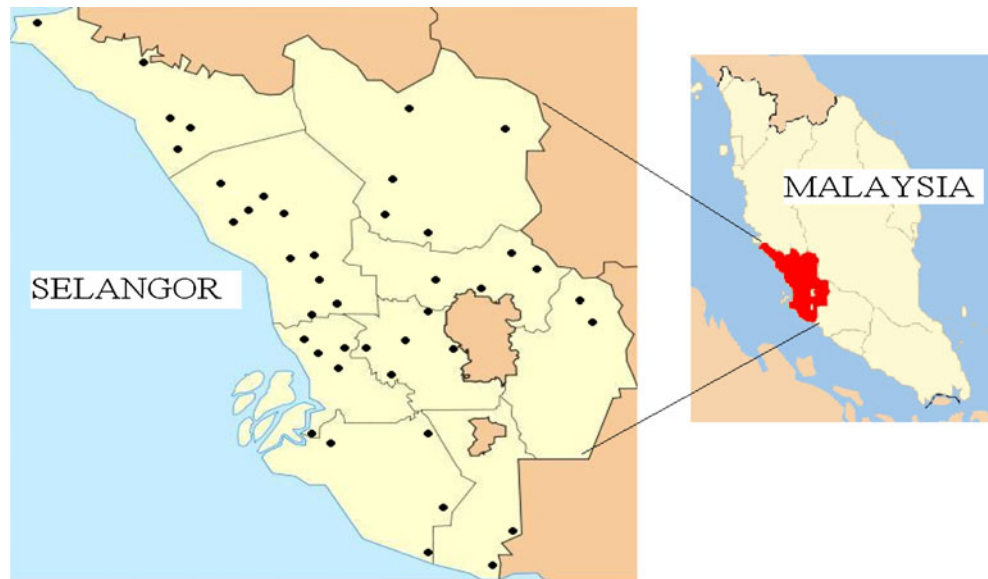
moments and TL-moments with regards to the three aforementioned probability distributions by first revisiting regional homogeneity establishment based on the L-moments by Hosking and Wallis (1997). Subsequently, corresponding relationships for regional homogeneity anal-

ysis and the regional parameters of the GEV and GLO distributions using TL-moments are developed. Annual maximum rainfall from 40 stations within Selangor, Malaysia, is utilized to perform the regional frequency analysis using both procedures.

Table 3 Station name and statistics of maximum daily rainfall for all the stations in Selangor

No	Name of station	Station number	n	Mean	Standard deviation	Kurtosis	Skewness	L-moments D_i	TL-moments D_i
1	Ldg. Batu Untong	2615131	37	132.76	35.639	-0.540	0.282	0.501	0.559
2	Ldg. Telok Merbau	2616135	37	105.9	34.983	2.144	1.025	0.287	0.702
3	Ldg. Sepang	2617134	35	103.863	31.949	-0.072	0.881	0.972	0.862
4	Ldg. Bute	2717114	37	95.908	26.609	-0.230	0.275	0.663	1.079
5	P.Kwln P.S T. Gong	2913001	33	119.788	76.604	21.328	4.246	0.620	0.294
6	Ldg. West	2913121	37	108.327	39.884	1.292	0.817	0.505	0.625
7	Jps. Pulau Lumut	2913122	37	98.03	34.085	0.902	0.882	0.232	1.009
8	Pejabat Jps. Klang	3014084	36	86.814	26.327	2.314	1.512	1.321	1.666
9	Ldg. Bukit Kerayong	3113059	37	108.587	99.032	31.629	5.450	3.167	0.802
10	Ldg. Sg. Kapar	3113087	37	105.114	30.082	-0.315	0.502	0.257	0.120
11	Ldg. Elmina	3115053	38	108.724	56.631	6.876	2.283	0.834	1.064
12	Sg. Buloh	3115079	38	94.097	29.121	0.175	0.414	0.350	0.990
13	Ldg. Edinburgh Station 2	3116006	31	95.326	22.588	-0.658	0.432	0.691	0.678
14	Pemasokan Ampang	3118069	22	103.014	35.893	0.988	0.314	1.853	1.615
15	Sek.Keb.Kg.Lui	3118102	37	114.654	61.209	2.426	1.599	1.704	2.860
16	Ldg. Braunston	3213057	34	91.832	33.297	0.026	0.769	0.837	1.411
17	Ldg. Bkt. Cherakah	3213058	38	96.982	69.306	27.097	4.830	1.225	0.424
18	Ldg. Bkt. Ijok	3214055	35	106.971	46.239	1.697	1.486	0.660	0.890
19	Kg. Sg. Tua	3216001	36	98.225	29.775	0.807	1.259	1.128	1.379
20	Ibu Bekalan Km. 16	3217001	36	97.258	21.489	1.339	0.401	3.187	2.195
21	Empangan G. Klang	3217002	36	100.306	38.42	11.265	2.716	0.272	0.988
22	Stn. Jenaletrik Lln.	3218101	37	108.257	56.682	2.921	1.636	1.401	1.925
23	Ldg. Bkt. Belimbing	3312042	36	97.828	40.173	3.722	1.918	0.576	0.848
24	Jln. Kelang	3312045	37	96.56	32.381	7.144	2.201	0.881	0.936
25	Ldg. Bkt. Talang	3313040	35	98.646	48.726	6.764	2.433	0.317	0.299
26	Ldg. Kuala Selangor	3313043	37	100.597	40.463	0.561	0.843	0.601	1.485
27	Ldg. Sg. Buloh	3313060	38	93.242	31.410	1.437	0.987	0.224	0.270
28	Rmh Pam Jps Jaya Setia	3314001	36	108.4	75.241	21.781	4.255	1.300	1.099
29	Ldg. Sg. Gapi	3316028	35	113.891	30.993	1.490	1.282	1.226	0.819
30	Genting Sempah	3317004	34	105.991	125.596	30.707	5.429	3.577	0.161
31	Parit 1 Sg. Burong	3411016	36	102.839	31.911	0.556	0.440	0.687	1.244
32	Ibu Bekalan Sg. Tengki	3412001	33	91.267	29.351	0.457	0.961	0.590	0.642
33	Ldg. Raja Musa	3412041	37	93.049	40.909	4.914	2.020	0.353	0.233
34	Ldg. Hopeful	3414030	35	109.254	36.913	0.145	0.940	1.025	2.030
35	Fdc. Sekichan	3510001	33	87.985	30.241	2.247	1.354	0.241	0.194
36	Parit 1 Sg. Besar	3609012	36	93.628	23.95	-0.109	0.559	0.619	2.427
37	Sg. Nipah	3610014	33	83.906	33.314	0.049	-0.228	3.949	1.645
38	Rumah Pam Jps Terap	3710006	37	86.527	22.678	0.044	0.364	0.513	0.816
39	Parit Sg. Air Tawar	3808001	33	89.924	39.671	2.672	1.538	0.426	0.554
40	Ldg Sg. Bernam	3809009	37	91.654	30.064	1.468	1.168	0.231	0.158

Fig. 1 Location of rain gauge stations used in study



2 TL-moments

The fundamental concepts of TL-moments are essentially the same as L-moments. Elamir and Seheult (2003) defined TL-moments as

$$\lambda_r^{(t)} = r^{-1} \sum_{k=0}^{r-1} (-1)^k \binom{r-1}{k} E(X_{r+t-k:r+2t})$$

where $E(X_{i:r}) = \frac{r!}{(i-1)!(r-1)!} \int_0^1 x(F)F^{i-1}(1-F)^{r-i} dF$

For $t=0$, TL-moments yields the original L-moments defined by Hosking (1990). For $t=1$, the first four TL-moments are expressed as

$$\lambda_1^{(1)} = E(X_{2:3}) = 6\beta_1 - 6\beta_2$$

$$\lambda_2^{(1)} = \frac{1}{2}E(X_{3:4} - X_{2:4}) = 6(-2\beta_3 + 3\beta_2 - \beta_1)$$

$$\begin{aligned} \lambda_3^{(1)} &= \frac{1}{3}E(X_{4:5} - 2X_{3:5} + X_{2:5}) \\ &= \frac{20}{3}(-5\beta_4 + 10\beta_3 - 6\beta_2 + \beta_1) \end{aligned}$$

$$\begin{aligned} \lambda_4^{(1)} &= \frac{1}{4}E(X_{5:6} - 3X_{4:6} + 3X_{3:6} - X_{2:6}) \\ &= \frac{15}{2}(-14\beta_5 + 35\beta_4 - 30\beta_3 + 10\beta_2 - \beta_1) \end{aligned}$$

The TL-moment ratios: TL-coefficient of variation (TL-Cv, $\tau_2^{(1)}$), TL-coefficient of skewness (L-Cs, $\tau_3^{(1)}$) and TL-coefficient of kurtosis (TL-Ck, $\tau_4^{(1)}$) are defined as

$$\tau_2^{(1)} = \frac{\lambda_2^{(1)}}{\lambda_1^{(1)}}, \tau_3^{(1)} = \frac{\lambda_3^{(1)}}{\lambda_2^{(1)}} \text{ and } \tau_4^{(1)} = \frac{\lambda_4^{(1)}}{\lambda_3^{(1)}}$$

Detailed discussions on L-moments and TL-moments can be found in numerous literatures such as Hosking (1990) and Elamir and Seheult (2003).

3 Regional frequency analysis based on L-moments

Hosking and Wallis (1993, 1997) organized regional frequency analysis into four stages: (a) screening of the data, (b) identifying homogeneous regions, (c) choosing a regional frequency distribution, and (d) estimating the regional frequency distribution. A discussion of the first three stages is given next.

Table 4 Moment ratios and parameter values of the fitted Kappa distribution

Method	Moment ratios			Parameters of the Kappa distribution			
	t_2^R	t_3^R	t_4^R	ξ Values	α Values	H values	K values
L-Moments	0.1946	0.2388	0.2055	0.8818	0.2046	-0.4735	-0.1886
TL-Moments	0.0953	0.1657	0.1065	0.9261	0.2012	-0.5179	-0.2494

Table 5 Results of the homogeneity test and goodness-of-fit test

Method	Homogeneity test			Z-test		
	H_1	H_2	H_3	GEV	GPA	GLO
L-Moment	-0.0618	-0.0650	-0.6679	-0.8055	-3.4530	0.2858
TL-Moment	-0.5072	-0.5812	-0.1876	-0.2929	-1.8514	0.0944

3.1 Discordance test

Discordancy test, D_i , is used to screen out data from stations whose point sample L-moments are markedly different from other stations. The objective is to check the suitability of the data for carrying out the regional analysis. The discordancy test, D_i , for station i is defined as

$$D_i = \frac{1}{3}N(u_i - \bar{u})^T S^{-1}(u_i - \bar{u})$$

$$S = \sum_{i=1}^N (u_i - \bar{u})(u_i - \bar{u})^T$$

where $u_i = [t_2^i \ t_3^i \ t_4^i]^T$ for station i , N is the number of stations, S is covariance matrix of u_i , and \bar{u} is the mean of vector, u_i . Critical values for discordancy statistic are tabulated by Hosking and Wallis (1993); for $N \geq 15$ stations, the critical value is 3. If the D -statistic of a station exceeds 3, its data is considered to be discordant from the rest of the regional data.

3.2 Heterogeneity test

An essential task in regional frequency analysis is the determination of homogeneous regions. Hosking and Wallis (1993) suggested the heterogeneity test, H , where L-moments are used to assess whether a group of stations may reasonably be treated as belonging to a homogeneous region. The proposed heterogeneity tests are based on: the L-coefficient of variation (L-Cv), the L-Cv and L-skewness (L-Cs); and L-Cs and L-kurtosis (L-Ck). These tests are defined respectively as

$$V_1 = \sqrt{\sum_{i=1}^N n_i (t_2^{(i)} - t_2^R)^2 / \sum_{i=1}^N n_i}$$

$$V_2 = \sum_{i=1}^N \left\{ n_i \left[(t_2^{(i)} - t_2^R)^2 + (t_3^{(i)} - t_3^R)^2 \right]^{1/2} \right\} / \sum_{i=1}^N n_i$$

$$V_3 = \sum_{i=1}^N \left\{ n_i \left[(t_3^{(i)} - t_3^R)^2 + (t_4^{(i)} - t_4^R)^2 \right]^{1/2} \right\} / \sum_{i=1}^N n_i$$

Here, the regional average L-moment ratios are calculated using the following formula

$$t_2^R = \sum_{i=1}^N n_i t_2^{(i)} / \sum_{i=1}^N n_i, t_3^R = \sum_{i=1}^N n_i t_3^{(i)} / \sum_{i=1}^N n_i$$

$$t_4^R = \sum_{i=1}^N n_i t_4^{(i)} / \sum_{i=1}^N n_i$$

where N is the number of stations and n_i is the record length at station i . The heterogeneity test is then defined as

$$H_j = (V_j - \mu_{V_j}) / \sigma_{V_j} \quad j = 1, 2, 3$$

where μ_{V_j} and σ_{V_j} are the mean and standard deviation of simulated V_j values, respectively. The estimated Kappa distribution is used to generate homogeneous regions with population parameters equal to the regional average sample L-moment ratios. Hosking and Wallis (1993, 1997) proposed the four parameters Kappa distribution in the simulation. The cumulative probability density function and quantile function for the Kappa distribution are

$$F(x) = \left\{ 1 - h \left[1 - \frac{k}{\alpha} (x - \xi) \right]^{1/k} \right\}^{1/h}$$

$$Q(F) = \xi + \frac{\alpha}{k} \left[1 - \left(\frac{1 - F^h}{h} \right)^k \right]$$

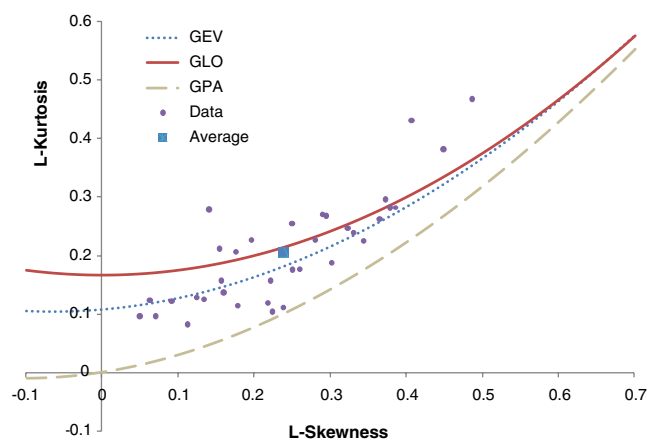


Fig. 2 L-moment ratio diagram of L-kurtosis versus L-skewness for annual maximum rainfall of the Selangor region

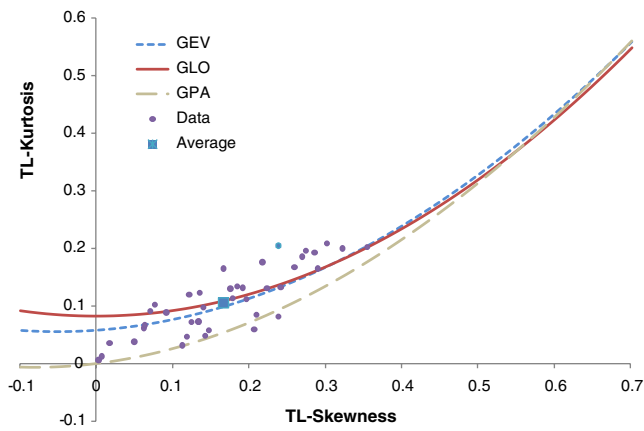


Fig. 3 TL-moment ratio diagram of L-kurtosis versus L-skewness for annual maximum rainfall of the Selangor region

The value of the *H*-statistic indicates that the region is acceptably homogeneous with a corresponding order of L-moments if $H < 1$, possibly homogeneous when $1 \leq H < 2$ and definitely heterogeneous when $H \geq 2$.

3.3 Selection of a regional frequency distribution

After confirming the homogeneity of the studied region, an appropriate distribution needs to be selected for the regional frequency analysis. Selection of the distribution is very crucial especially for relatively large return periods because the distribution type can affect, to a great extent, the magnitude of the estimated floods. The L-moment ratio diagram and Z-test are employed for this purpose.

The L-moment ratio diagram is a graph of the L-Cs and L-Ck which compares the fit of several distributions on the same graph. However, direct visual inspection of the L-moment ratio diagram is somewhat subjective as more than one distribution could pose as a possible candidate.

The Z-test judges how well the simulated L-Cs and L-Ck of a fitted distribution matches the regional average L-Cs and L-Ck values. For each selected distribution, the Z-test is calculated as follows

$$Z^{DIS} = (\tau_4^{Dis} - t_4^R) / \sigma_4$$

where *DIS* refers to a particular distribution, τ_4^{Dis} is the L-kurtosis of the fitted distribution while the standard deviation of t_4^R is given by

$$\sigma_4 = \left[(N_{sim})^{-1} \sum_{m=1}^{N_{sim}} (t_4^{(m)} - t_4^R)^2 \right]^{1/2}$$

$t_4^{(m)}$ is the average regional L-kurtosis and has to be calculated for the *m*th simulated region. This is obtained by simulating a large number of kappa using Monte Carlo simulations. The value of the Z-statistics is considered to be acceptable at the 90% confidence level if $|Z^{DIS}| \leq 1.64$. If more than one candidate distribution is acceptable, the one with the lowest $|Z^{DIS}|$ is regarded as the best-fit distribution.

Details on the method of L-moments in estimating the parameters of several distributions can be found in Sankarasubramaniam and Srinivasan (1999).

4 Regional frequency analysis based on TL-moments

The procedures discussed in Section 3 are similarly employed for the TL-moments. The L-Cv, L-Cs, and L-Ck are equally replaced by the TL-Cv, TL-Cs, and TL-Ck for the discordancy and the homogeneity test. Selection of an adequately fitted distribution is carried out based on the TL-ratio diagram and Z-test using the regional TL-Cs and TL-Ck. As discussed before, distribution whose absolute Z-test value is less than 1.64 qualify as the possible candidate, the best distribution being the one with the lowest value. Formulas for the TL-Cv, TL-Cs, and TL-Ck are as discussed in Section 2.

Estimation of the design floods for specific return periods are generally needed in flood studies. Presently, of the three distributions under consideration, TL-moment parameter estimates are only available for the GPA distribution. In this research, TL-moment parameter estimates of GEV and GLO are developed and used to test for robustness of the distributions. Table 1 shows the TL-moments, TL-moment ratios, and the associated

Table 6 Regional parameter and quantile estimates of the GEV and GLO distributions for L-moments and TL-moments

Method	Distribution	ξ Value	α Value	<i>k</i> Value	Q ₂	Q ₅	Q ₁₀	Q ₂₀	Q ₅₀	Q ₁₀₀
L-Moments	GLO	0.926	0.177	-0.239	0.926	1.217	1.438	1.682	2.063	2.406
	GEV	0.825	0.252	-0.105	0.919	1.234	1.465	1.703	2.040	2.315
TL-Moments	GLO	0.964	0.180	-0.298	0.964	1.273	1.523	1.813	2.286	2.735
	GEV	0.870	0.241	-0.162	0.961	1.279	1.524	1.789	2.181	2.517

Table 7 RBIAS values for different quantiles of the GEV and GLO distributions for L-moments and TL-moments

Sample size (<i>n</i>)	Method	Distribution	Q ₂	Q ₅	Q ₁₀	Q ₂₀	Q ₅₀	Q ₁₀₀
20	L-Moments	GLO	-0.003	0.007	0.011	0.011	0.004	-0.009
		GEV	-0.003	0.005	0.009	0.009	0.002	-0.010
	TL-Moments	GLO	-0.002	0.006	0.003	-0.009	-0.046	-0.094
		GEV	-0.002	0.006	0.002	-0.013	-0.059	-0.119
50	L-Moments	GLO	-0.001	0.003	0.004	0.004	0.001	-0.005
		GEV	-0.001	0.002	0.004	0.004	0.001	-0.005
	TL-Moments	GLO	-0.001	0.002	0.001	-0.003	-0.015	-0.030
		GEV	-0.000	0.002	-0.001	-0.008	-0.026	-0.047
80	L-Moments	GLO	-0.001	0.002	0.003	0.003	0.000	-0.003
		GEV	-0.001	0.001	0.002	0.002	-0.000	-0.004
	TL-Moments	GLO	-0.000	0.001	0.000	-0.002	-0.010	-0.020
		GEV	-0.000	0.001	-0.001	-0.007	-0.019	-0.032

parameters derived for the GEV, GPA, and GLO distributions. Table 2 shows the coefficients for the newly developed relationships of TL-Cs and TL-Ck of the GPA, GEV, and GLO distributions based on TL-moments for the range $-1 \leq \tau_3^{(1)} \leq 1$.

5 Case study

Records of daily rainfall from 40 stations in Selangor with record lengths of 22 to 38 years were acquired from the Department of Irrigation and Drainage, Malaysia. The statistics and basic information of the data are listed in Table 3. All the stations, numbered 1 to 40, are located throughout Selangor with latitudes ranging from 26° up to 38° and longitudes from 8° to 18°, as shown in Fig. 1.

6 Results and discussions

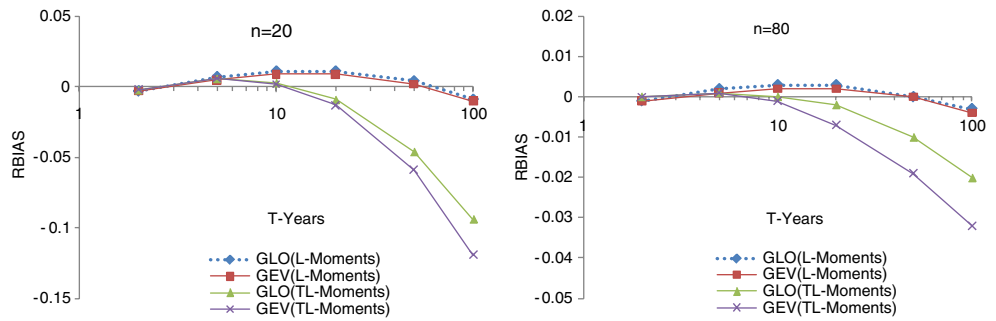
Initially, the whole of Selangor was assumed as one homogeneous region, and the discordancy test was used for data verification and quality control. Results of the discordancy test, D_i , are given in Table 3. It is observed that, for the L-moments method, $D_{critical}=3.0$, is exceeded at four locations: stations 9, 20, 30, and 37, with D -statistic values of 3.167, 3.187, 3.577, and 3.949, respectively. Therefore, these four stations are excluded from the regional frequency analysis.

However, for the TL-moments method, it is observed that the D -statistic values for the 40 stations vary from 0.120 to 2.860. The largest D -statistic value is 2.860 for station 15, hence none of the stations have a D -statistic exceeding the critical value. Thus, for the TL-moments method, data from all stations are used for the development of regional frequency analysis.

Table 8 RRMSE values for different quantiles of the GEV and GLO distributions for L-moments and TL-moments

Sample size (<i>n</i>)	Method	Distribution	Q ₂	Q ₅	Q ₁₀	Q ₂₀	Q ₅₀	Q ₁₀₀
20	L-Moments	GLO	0.078	0.095	0.125	0.169	0.252	0.337
		GEV	0.083	0.098	0.120	0.155	0.222	0.289
	TL-Moments	GLO	0.030	0.047	0.106	0.190	0.355	0.541
		GEV	0.028	0.046	0.102	0.186	0.354	0.549
50	L-Moments	GLO	0.049	0.060	0.081	0.112	0.166	0.217
		GEV	0.052	0.062	0.077	0.100	0.142	0.182
	TL-Moments	GLO	0.018	0.029	0.066	0.113	0.194	0.270
		GEV	0.017	0.029	0.063	0.110	0.192	0.272
80	L-Moments	GLO	0.039	0.048	0.065	0.089	0.132	0.172
		GEV	0.041	0.049	0.061	0.079	0.113	0.144
	TL-Moments	GLO	0.014	0.023	0.052	0.089	0.149	0.205
		GEV	0.013	0.022	0.049	0.086	0.146	0.203

Fig. 4 Results of the RBIAS for sample sizes 20 and 80 computed for quantile $T=2, 5, 10, 20, 50,$ and 100 years



The regional average L-moment ratios and average TL-moment ratios of the respective study regions are calculated, and the corresponding parameter values of the fitted Kappa distribution are found as presented in Table 4.

The H-statistics are computed by carrying out 500 simulations using the Kappa distribution based on the data from 36 stations for the L-moments and 40 stations for the TL-moments. Results of the H-tests for the L-moments and TL-moments, as given in Table 5, indicate that the study region demonstrates acceptable homogeneity ($H < 1$), therefore a subdivision of the stations into more regions was not necessary.

After confirming the homogeneity of the study region, an appropriate distribution needs to be selected for the regional frequency analysis. Figures 2 and 3 show a comparison of the observed and theoretical relations between the L-moments and the TL-moments, respectively. In the L-moment ratio diagram of Fig. 2, the point defined by the sample average values of $t_3^R = 0.2388$ and $t_4^R = 0.2055$, lies closest to the L-moments of the GLO distribution followed by GEV and GPA distributions.

Analysis of the TL-moment ratio diagram reveals that the sample average values of $t_3^{R(1)} = 0.1657$ and $t_4^{R(1)} = 0.1065$ in the diagram are better described by the theoretical TL-moments of the GLO and GEV rather than the GPA, hence the GLO and GEV distributions should be preferred.

Results of the Z-test for the three distributions are given in Table 5. For both the L-moments and TL-moments methods, the GPA distribution failed the test with a Z-test

exceeding the critical value of 1.64. However, the GLO should be considered as the best-fit distribution, as this distribution gives the minimum Z-test for both the L-moments and TL-moments methods.

In regional frequency analysis, the final and important objective is to determine the robustness of the distribution in producing reasonably reliable estimates at all stations in the homogeneous region. Regional flood frequency relationships are developed using the chosen GLO and GEV distributions. The form of the regional frequency relationship or the growth factor for GLO and GEV distributions are respectively

$$Q_T = \xi + \frac{\alpha}{k} \left\{ 1 - \left(\frac{1}{T-1} \right)^k \right\}$$

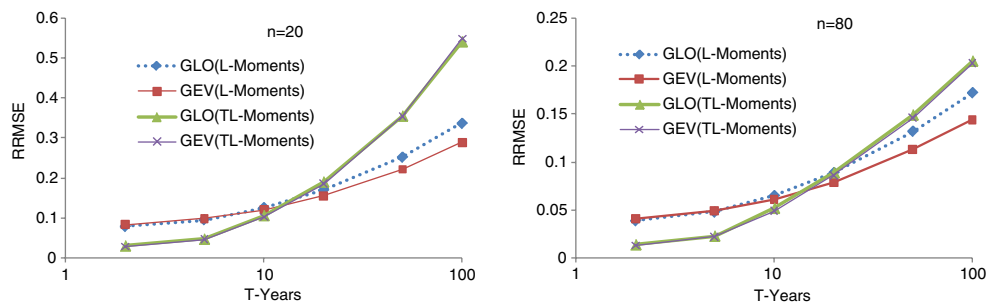
and

$$Q_T = \xi + \frac{\alpha}{k} \left\{ 1 - [-\log(1 - 1/T)]^k \right\}$$

where Q_T is quantile estimation at T -years return period. The regional parameters and the quantiles estimated for the GLO and GEV distributions for $T=2, 5, 10, 20, 50,$ and 100 years, using L-moments and TL-moments, are presented in Table 6.

The robustness of the designated regional frequency distributions is further investigated for estimation of design flood quantiles. For this purpose, Meshgi and Khalili (2009) proposed Monte Carlo simulation to evaluate the

Fig. 5 Results of the RRMSE for sample sizes 20 and 80 computed for quantiles $T=2, 5, 10, 20, 50,$ and 100 years



errors between the simulated and calculated design flood quantiles. Two measures of performance that were used are the relative bias (RBIAS) and the relative root mean square error (RRMSE)

$$RBIAS = M^{-1} \sum_{m=1}^M \frac{Q_T^{(m)} - Q_T^C}{Q_T^C}$$

$$RRMSE = \sqrt{M^{-1} \sum_{m=1}^M \left(\frac{Q_T^{(m)} - Q_T^C}{Q_T^C} \right)^2}$$

where M is the sample size, $Q_T^{(m)}$ and Q_T^C is the simulated and true quantile of design flood at T -years, respectively.

Tables 7 and 8 present the RBIAS and RRMSE values of quantiles computed using the L-moments and TL-moments for the GEV and GLO distributions. Figures 4 and 5 provide the results of the RBIAS and the RRMSE for sample sizes of 20 and 80, respectively.

The results show that the RBIAS and RRMSE values generally increase with a reduction in the sample size and for prediction of larger quantiles. The GEV distribution performs better than GLO distribution for the L-moments. However, the performances of GEV and GLO distributions are approximately similar for the TL-moments. Interestingly, the TL-moments method is significantly more efficient than the L-moments method for return periods, T , of less than 10 years. However, the performance of the L-moments method supercedes that of the TL-moments for higher return periods.

7 Conclusion

The study provides a comprehensive evaluation of the L-moments and TL-moments, by first revisiting regional frequency analysis based on the L-moments by Hosking and Wallis (1993; 1997). Regional homogeneity was investigated by first assuming the entire study area as one homogeneous regional cluster. The corresponding relationships for regional homogeneity analysis by the TL-moments are developed. TL-moments for the GPA, GLO, and GEV distributions are also developed and used to provide the corresponding TL-moment ratio diagrams and the goodness-of-fit test.

The results of this study have shown that, from 40 stations in the study region, 36 stations based on L-moments and all stations based on TL-moments are accepted statistically to be homogeneous using the discordancy test and heterogeneity test. The Z-test has also shown that the L-moments and TL-moments method produced the same results, where GLO and GEV were identified as the

best distributions for modeling daily annual maximum rainfall in Selangor, Malaysia. Finally, Monte Carlo simulations which are used for performance evaluation showed that the TL-moments method is more efficient for lower quantile estimation but the L-moments method does outperform for higher quantile estimations.

References

- Abida H, Ellouze M (2008) Probability distribution of flood flows in Tunisia. *Hydrol Earth Syst Sci* 12:703–714
- Cannarozzo M, Noto LV, La Loggia G (2009) Annual runoff regional frequency analysis in Sicily. *Phys Chem Earth* 34:679–687
- Chen YD, Huang G, Shao Q, Xu CY (2006) Regional analysis of low flow using L-moments for Dongjiang basin, South China. *Hydrol Sci J des Sci Hydrol* 51(6):1051–1064
- Elamir EA, Seheult AH (2003) Trimmed L-moments. *Comput Stat Data Anal* 43:299–314
- Fowler HJ, Kilsby CG (2003) A regional frequency analysis of United Kingdom extreme rainfall from 1961 to 2000. *Int J Climatol* 23:1313–1334
- Glaves R, Waylen PR (1997) Regional flood frequency analysis in Southern Ontario using L-moments. *Can Geogr* 41(2):178–193
- Hosking JRM (1990) L-Moments: Analysis and estimation of distributions using linear combinations of order statistics. *J Royal Statistical Society B* 52:105–124
- Hosking JRM, Wallis JR (1993) Some statistics useful in regional frequency analysis. *Water Resour Res* 29(2):271–281
- Hosking JRM, Wallis JR (1997) Regional frequency analysis: An approach based on L-moments. University press, Cambridge
- Hussain Z, Pasha GR (2009) Regional flood frequency analysis of the seven stations of Punjab, Pakistan, using L-moments. *Water Resour Manage* 23(10):1917–1933
- Jingyi Z, Hall MJ (2004) Regional flood frequency analysis for the Gan-Ming River basin in China. *J Hydrol* 296:98–117
- Kjeldsen TR, Smithers JC, Schulze RE (2002) Regional flood frequency analysis in the KwaZulu-Natal province, South Africa using the index-flood method. *J Hydrol* 255:194–211
- Kumar R, Singh RD, Seth SM (1999) Regional flood formulas for seven subzones of zone 3 of India. *J Hydrol Eng* 4(3):240–244
- Kumar R, Chatterjee C, Panigrihy N, Patwary BC, Singh RD (2003) Development of regional flood formulae using L-moments for gauged and ungauged catchments of North Brahmaputra river system. *J Inst Eng (India) Civil Eng Div* 84(1):57–63
- Kysely J (2009) Trends in heavy precipitation in the Czech Republic over 1961–2005. *Int J Climatol* 29:1745–1758
- Lim YH, Lye LM (2003) Regional flood estimation for ungauged basins in Sarawak, Malaysia. *Hydrol Sci J* 48(1):79–94
- Madsen H, Rasmussen PF, Rosbjerg D (1997) Comparison of annual maximum series and partial duration series methods for modeling extreme hydrologic events. 2. Regional modelling. *Water Resour Res* 33(4):759–769
- Meshgi A, Khalili D (2009) Comprehensive evaluation of regional flood frequency analysis by L- and LH-moments. II. Development of LH-moments parameters for the generalized Pareto and generalized logistic distributions. *Stoch Environ Res Risk Assess* 23:137–152

- Noto LV, La Loggia G (2009) Use of L-moments approach for regional frequency analysis in Sicily Italy. *Water Resour Manag* 1:23
- Parida BP, Kachroo RK, Shrestha DB (1998) Regional flood frequency analysis of Mahi-Sabarmati Basin (Subzone 3-a) using index flood procedure with L-moments. *Water Resour Manage* 12:1–12
- Rahnama MB, Rostami R (2007) Halil-Basin regional flood frequency analysis based on L-moment approach. *Int J Agric Res* 2(3):261–267
- Saf B (2010) Regional flood frequency analysis using L-moments for the West Mediterranean region of Turke. *Water Resour Manage* 23(3):531–551
- Sankarasubramaniam A, Srinivasan K (1999) Investigation and comparison of sampling properties of L-moments and conventional moments. *J Hydrol* 218:13–34
- Yue S, Wang C (2004) Determination of regional probability distributions of Canadian flood flows using L-moments. *J Hydrol NZ* 43(1):59–73
- Zalina MD, Nguyen V-T-V, Amir MK, Mohd Nor MD (2002) Selecting a probability distribution for extreme rainfall series in Malaysia. *Water Sci Technol J* 45(2):63–68
- Zin WZW, Jemain AA, Ibrahim K (2009) The best fitting distribution of annual maximum rainfall in Peninsular Malaysia based on methods of L-moment and LQ-moment. *Theor Appl Climatol* 96:337–344